Electronic Supplementary Material (ESI) for RSC Advances.

Supporting Information

A novel energy efficient path for nitrogen fixation using non-thermal arc

Iqbal Muzammil, Dae Hoon Lee,* Duy Khoe Dinh, Hongjae Kang, Seon Ah Roh, You-Na Kim, Seongil Choi, Chanmi Jung, Young-Hoon Song

Department of Environmental and Energy Systems, Korea Institute of Machinery and Materials, 156 Gajeongbuk-Ro, Yuseong-Gu, Daejeon, South Korea

*Corresponding author. Email: dhlee@kimm.re.kr

Contents

S.1 Current and voltage characteristics

Figure S1 shows the influence of the air flow rate on the voltage–current signal for the RGA reactor at 200 W. The small increase in the average voltage of the arc igniter indicates that the arc length does not change significantly with change in the flow rate. As the air flow rate increases, the fluctuation in the voltage–current signal increases continuously. At a low flow rate of 20 L/min, when Re is approximately 1837, the flow inside the reactor is in the laminar flow regime and the relatively small aerodynamic force causes only discernible flow-induced fluctuations of the current flow inside the arc. However, at a high flow rate, when Re is 13,780, and the flow is in a highly turbulent regime, the flow-induced fluctuation of the current is relatively stronger, resulting in a shorter arc shunt period (shorter arc length). The full width at half maximum (FWHM) of a single discharge arc current at 20 L/min is 0.3 μs, whereas it is 0.12 μs at 150 L/min.

In addition to the arc region, the plasma jet length is also influenced significantly by the gas flow rate. At the gas flow rate of 20 L/min, the plasma jet has a longer length than that at the gas flow rate of 150 L/min. The high jet flow rate induces strong entrainment of the ambient air surrounding the jet, resulting in faster mixing of the jet with the ambient air, which reduces the density of the excited species and creates less reactive flow conditions at the exit of the reactor.

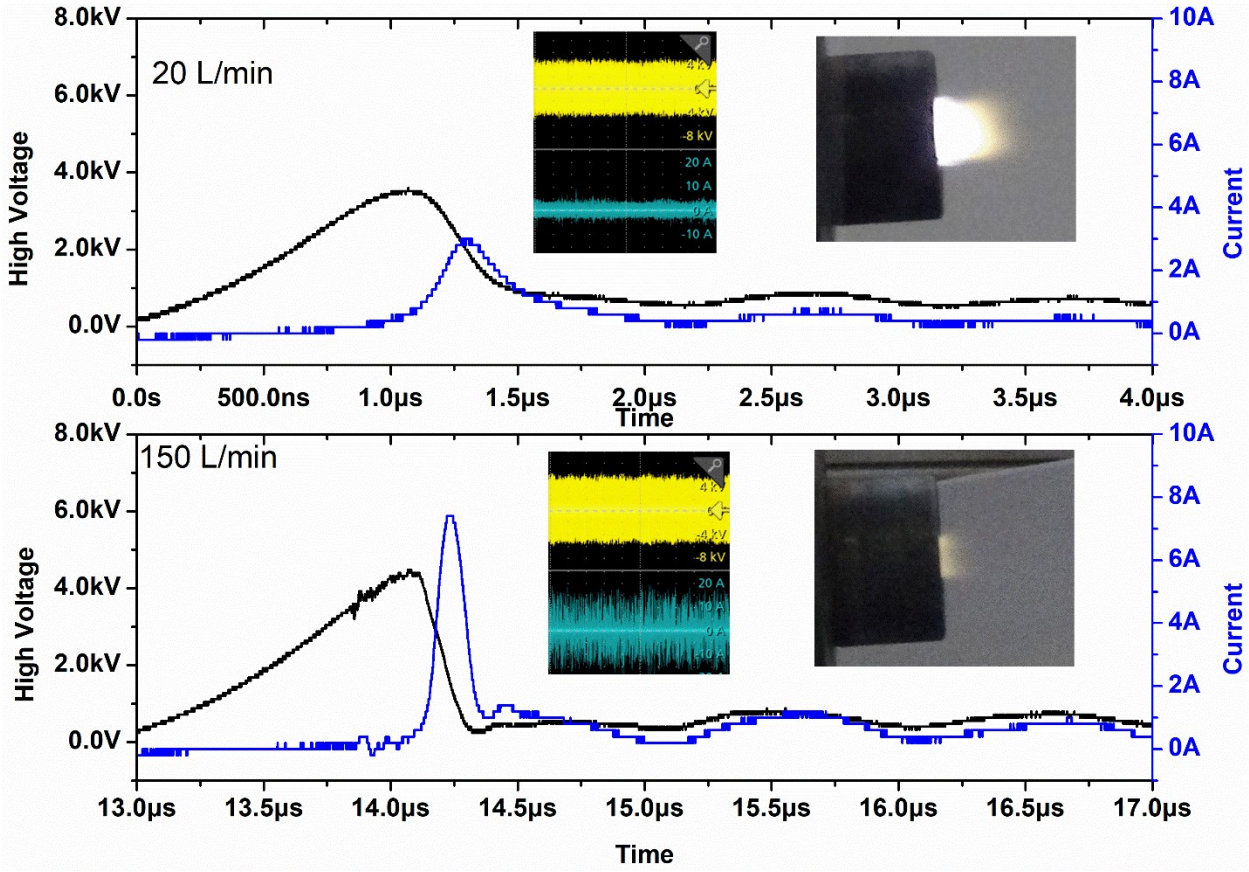

Figure S1. Voltage–current signal of the rotating arc plasma reactor at 30 µs/div for the air flow rate of (a) 20 L/min and (b) 150 L/min. Insets in each graph are the plasma jet images and oscillograms representing the voltage and current characteristics of the stably elongated arc, having an overall time span of 0.1 s.

S.2 Reaction mechanism for high NO selectivity

In situ Fourier transform infrared (FTIR) analyses were performed on the gas product. The FTIR spectrometer was equipped with liquid-nitrogen-cooled mercury–cadmium–telluride detector with a resolution of 0.5 cm^{-1}. The spectrum of each trial is based on an average of 32 spectra. The NO and NO_2 concentrations were calibrated with a series of standard calibrated gases for NO (3%, 1%,

and 0.5%) and NO_2 (0.5%, 0.1%, and 0.01%). The following vibrational bands were used as diagnostics for the presence of various nitrogen oxides species: N_2O at 610, 665, 1282, and 3558 cm^{-1}; N_2O_5 due to deformations of NO_2 at 770 cm^{-1}; N_2O_4 due to NO stretching at 1240, 1690, and 1713 cm^{-1}; NO at 1840 and 1911 cm^{-1}; NO_2 at 1590, 1629, and 2917 cm^{-1}.[1–4] The relationship between the absorbance and concentrations of the various standard NO gases (3%, 1%, and 0.5%) between the peaks at 1840 and 1911 cm^{-1} remained linear. The relationship between the absorbance and NO_2 concentration between the peaks at 1590 and 1629 cm^{-1} was nonlinear, whereas the peaks went out of range beyond 500 ppm. A discussion on the non-linearity phenomenon in the FTIR gas-phase spectroscopy for higher concentration is previously reported. [5] Therefore, all the NO_2 concentrations were measured by a weak vibrational band at 2917 cm^{-1} and these show good agreement with the measurements of standard calibrated gases.

Figure S2 shows the FTIR spectra of NO_x generated during RGA discharges in the air for various flow rates.

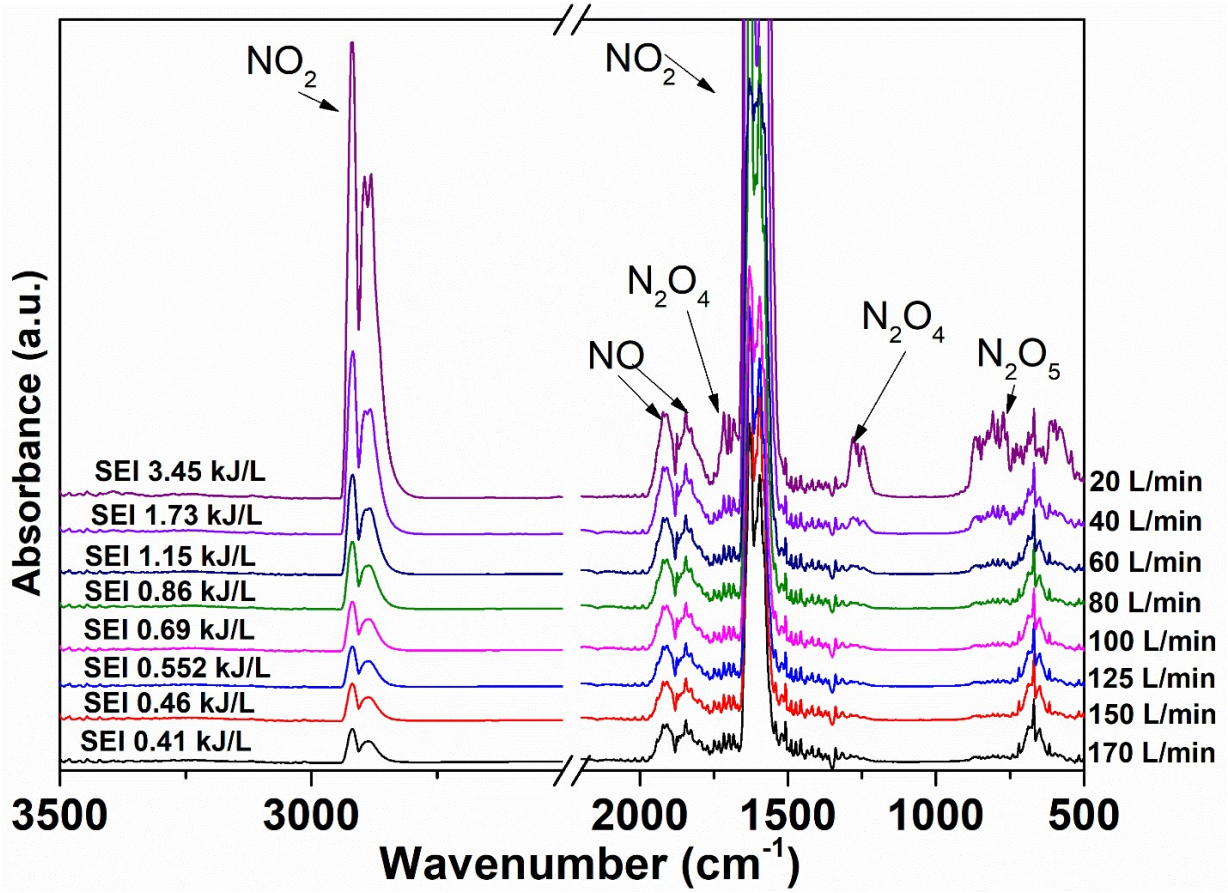

Figure S2. Fourier transform infrared spectra at various specific energy inputs.

This NO_x concentration includes only NO and NO_2 (N_2O, N_2O_4, and N_2O_3 are not included). However, at low flow rates and high SEI conditions, the spectra show that various nitrogen oxide species, such as N_2O, N_2O_4, and N_2O_3 are present; but their concentrations were low. The 0D model in previous work confirmed presence of other nitrogen oxide is low.[6] The following nitrogen fixation reactions from air plasma have been suggested:

$$e + O_2 \rightarrow O + O + e, \quad (1)$$

$$e + N_2 \rightarrow N + N + e, \quad (2)$$

$$N_2 + O \rightarrow NO + N \quad (3)$$

$$N + O_2 \rightarrow NO + O, \quad (4)$$

$$N + NO \rightarrow N_2 + O, \quad (5)$$

$$O^* + NO \rightarrow N_2 + O_2, \quad (6)$$

$$NO + O + M \rightarrow NO_2 + M, \quad (7)$$

$$O + NO_2 \rightarrow NO + O_2, \quad (8)$$

$$NO + NO_3 \rightarrow 2NO_2, \quad (9)$$

$$NO_2 + NO_3 \rightarrow N_2O_5, \quad (10)$$

$$N_2O_5 \rightarrow NO_2 + NO_3, \quad (11)$$

$$O + N_2O_5 \rightarrow 2NO_2 + O, \quad (12)$$

$$N_2^* + NO \rightarrow N_2 + N + O. \quad (13)$$

In Reactions 1 and 2, the energetic electrons produced in the plasma reactor decompose the N_2 and O_2 molecules into N and O atoms, respectively, and form NO during Reaction 3 and 4. The main contribution for NO formation comes from Reaction 3, because of much easier dissociation of O_2 (Reaction 1) than N_2 molecules (Reaction 2). The bond dissociation energy of the O_2

molecule is 5.15 eV and N_2 molecules is 9.79 eV.[6] Then, the NO remaining in the reaction volume may cause a drop in the NO production, as indicated by Reactions 5 and 6. Meanwhile, the O radicals react with NO to form NO_2 through Reaction 7; therefore, it is essential to stop the reaction quickly to avoid further oxidation for higher NO selectivity. NO is regenerated from NO_2 through Reaction 8. Reactions 9 to 13 change the NO_x compositions and decrease the selectivity of NO_x, but the total NO_x concentration remains the same. Therefore, it is crucial to control the condition inside the plasma reaction volume to obtain higher NO_x selectivity.

To avoid these redundant reactions under high-temperature condition, the air flow rate is increased; this not only decreases the thermal loss but also helps to quench the reaction faster. Surprisingly, energy-efficient NO_x with 95% NO selectivity is obtained, and all other nitrogen oxide species vanish owing to the quenching of redundant reactions under high flow rate and low SEI.

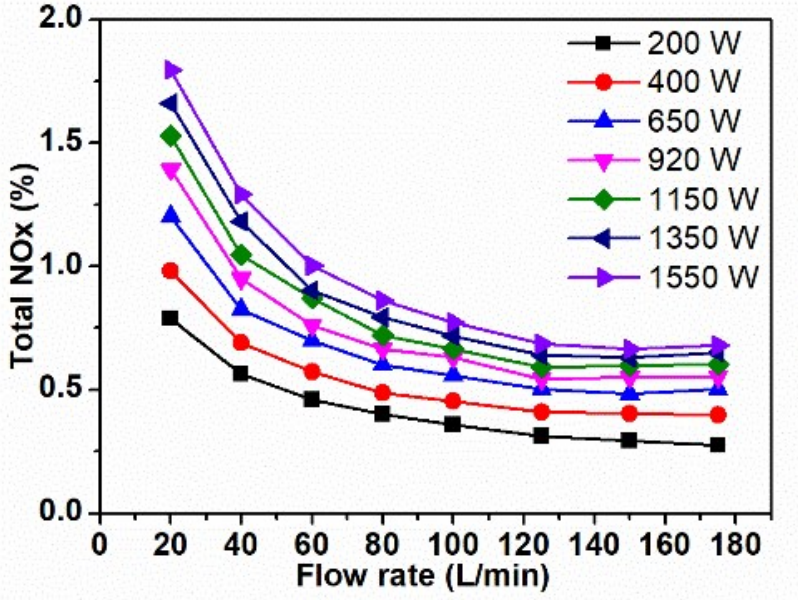

(a) Total NOx production

(b) NO selectivity

(c) Energgy consumption

Figure S3. (a) Total NO_x production, (b) NO selectivity, and (c) energy consumption as functions of the air flow rate at various powers.

Experiments were conducted using different input power condition between 200 and 2000 W and air flow rates between 20 and 170 L/min. As shown in Figure S3, the increase in the electrical energy is beneficial for increasing the NO_x production; NO_x concentration of 1.8% is achieved at the power of 1550 W and flow rate of 20 L/min.

References

[1] A.L.F. de Barros, E.F. da Silveira, D. Fulvio, P. Boduch, H. Rothard, Formation of nitrogen-and oxygen-bearing molecules from radiolysis of nitrous oxide ices–implications for Solar system and interstellar ices, Mon. Not. R. Astron. Soc. 465 (2016) 3281–3290.

[2] C.S. Jamieson, C.J. Bennett, A.M. Mebel, R.I. Kaiser, Investigating the Mechanism for the Formation of Nitrous Oxide [N2O (X 1Σ+)] in Extraterrestrial Ices, Astrophys. J. 624 (2005) 436.

[3] D. Fulvio, B. Sivaraman, G.A. Baratta, M.E. Palumbo, N.J. Mason, Novel measurements of refractive index, density and mid-infrared integrated band strengths for solid O2, N2O and NO2:N2O4 mixtures, Spectrochim. Acta - Part A Mol. Biomol. Spectrosc. 72 (2009) 1007–1013. doi:10.1016/j.saa.2008.12.030.

[4] G.C. Almeida, S. Pilling, A.L.F. de Barros, C.A.P. da Costa, R.C. Pereira, E.F. da Silveira, Processing of N2O ice by fast ions: Implications on nitrogen chemistry in cold astrophysical environments, Mon. Not. R. Astron. Soc. 471 (2017) 1330–1340.

doi:10.1093/mnras/stx1438.

[5] M. Ahro, J. Kauppinen, Nonlinearity of Beer's law in gas-phase FT-IR spectroscopy, Appl. Spectrosc. 55 (2001) 50–54. doi:10.1366/0003702011951425.

[6] E. Vervloessem, M. Aghaei, F. Jardali, N. Hafezkhiabani, A. Bogaerts, Plasma-based N_2 fixation into NO_x: Insights from modeling toward optimum yields and energy costs in a gliding arc plasmatron, ACS Sustain. Chem. Eng. (2020) acssuschemeng.0c01815. doi:10.1021/acssuschemeng.0c01815.